

Electronic Mechanism for Production of Self-Phase Modulation

R. R. Alfano, L. L. Hope, and S. L. Shapiro

Bayside Research Center, GTE Laboratories Incorporated, Bayside, New York 11360

(Received 20 December 1971)

Characteristics of self-phase-modulation (SPM) spectra observed when intense picosecond pulses are passed through liquids and solids are shown to be consistent with a theoretical model based on an electronic mechanism. Experimental observations and theoretical calculations show that the SPM mechanism must respond on a subpicosecond scale.

INTRODUCTION

An intense optical pulse propagating through a material can distort the atomic configuration and change the refractive index appreciably. The index change can be caused by direct distortion of the electronic clouds, by forced diffusional, rotational, or librational motion of atoms or atomic clusters, or by a coupled mechanism. The index acquires a time dependence, so that the phase of the optical wave is altered, leading in general to broadening of the pulse spectrum. This process has been called self-phase modulation (SPM). Spectral broadening was first observed in CS_2 by Brewer¹ and interpreted in terms of SPM by Shimizu,² who attributed the broadening resulting when a 20-nsec Q -switched ruby-laser pulse passed through CS_2 to the orientational Kerr effect. Libration of the CS_2 molecules has also been proposed to explain these spectra.³ Brewer and Lee⁴ observed self-focusing of picosecond laser pulses in CS_2 and viscous liquids, and suggested that the index nonlinearity is of electronic origin. Recently, Alfano and Shapiro,⁵ using picosecond pulses at 5300 \AA , have observed SPM and self-focusing in various crystals, liquids, and glasses, including liquefied and solidified rare gases. They showed that the electronic mechanism for SPM is important in all materials and dominates all other processes in some materials, e. g., liquid argon and krypton. The electronic part of the nonlinear index of CCl_4 has been deduced to be 54%⁶ using 20-nsec laser pulses. They have also observed three nonlinear optical effects generated within picosecond-

emitting lasers.⁵ The electronic distortion mechanism is of course present in all material, a fact consistent with experimental observation of SPM spectra in all samples studied under intense picosecond excitation.⁵ In this paper, experimental and theoretical evidence is presented supporting the direct-electronic-distortion model of SPM.

EXPERIMENT

A typical experimental arrangement is shown in Fig. 1. The mode-locked Nd:glass laser is described in earlier papers.⁵ A fraction of the laser output at 1.06μ is converted to second harmonic at 0.53μ . The harmonic radiation consists of pulses of about 2×10^8 -W power and 4-psec duration. The beam is collimated by an inverted telescope and enters the sample with a beam diameter of about 1.2 mm. The intensity distribution at the exit face of the sample is magnified and imaged either on the 1-mm slit of a Jarrel-Ash $\frac{1}{2}$ -m grating spectrograph, a 2-m Bausch and Lomb spectrograph, or a prism spectrograph, so that the spectrum of each filament is displayed. A combination of a 3-mm wire placed at the focal point of the imaging lens and/or Corning filters (Stokes side 3-67, 3-68, anti-Stokes side 5-60, 5-61) is used to prevent any laser light that has not formed filaments from entering the spectrograph.^{2,5}

Typical SPM spectra from various solids and liquids are shown in Fig. 2: calcite, liquid carbon tetrachloride, liquid nitrogen, liquid argon, and solid krypton. These spectra are characterized by very large spectral widths and a nonperiodic or random substructure. Occasionally, a periodic structure of

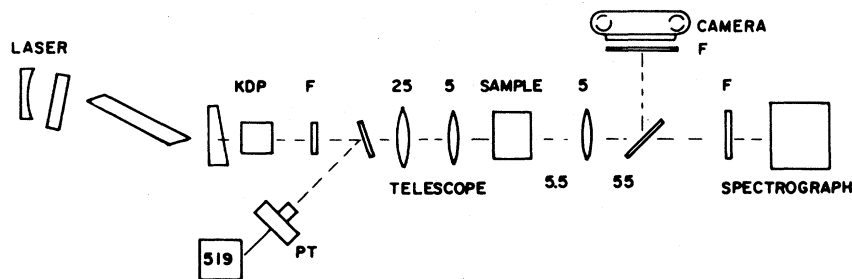


FIG. 1. Typical experimental arrangement for the observation of SPM.

interference minima and maxima are observed. The modulation frequencies range from a few cm^{-1}

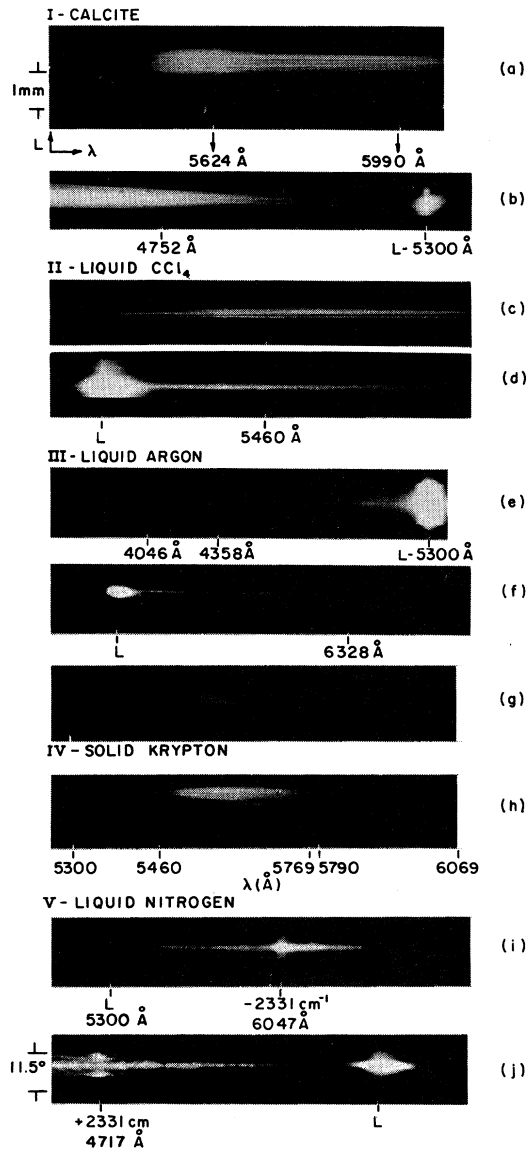


FIG. 2. SPM spectra observed when intense, 5300-Å, psec laser pulses are passed through the following material. I: Calcite—length $l=5$ cm. (a) Stokes filter $F(2, 3-67)$ and (b) anti-Stokes $F(2, 5-60)$ spectra. II: Liquid CCl_4 — $l=4$ cm. (c) Stokes $F(4, 3-68)$ and (d) Stokes $F(1, 3-68)$ spectra. III: Liquid argon— $l=12$ cm. (e) anti-Stokes $F(5-61)$, (f) Stokes, $F(3-67)$, and (g) Stokes $F(3, 3-67)$ spectra. The beam is focused into the sample with $f=25$ -cm lens (the beam diameter is measured to be $\sim 300 \mu$ at the focal point); IV: Solid krypton— $l=12$ cm. (h) Stokes $F(3, 3-67)$ spectra. The beam is focused with $f=25$ -cm lens. V: Liquid nitrogen— $l=7$ cm. (i) Stokes $F(3-67)$ and (j) anti-Stokes $F(5-60, 5-61)$ angular emission spectra. Photograph (i) displays stimulated Raman emission and axial SPM and (j) displays an anti-Stokes ring and axial SPM.

to hundreds of cm^{-1} , and for some, observations progressively increase away from the central frequency.

For spectra of less than about 5000-cm^{-1} total width, the spectral extents on the Stokes and anti-Stokes sides are the same within 20%. The Stokes and anti-Stokes spectra are approximately equal in intensity and roughly the peak intensity at the central frequency is $\sim 10^2\text{--}10^3$ the intensity of the SPM spectra at a given frequency. These results were verified with a prism spectrometer, so that the intensity calibration problems inherent in other instruments were avoided. The spectra also appeared symmetric about the input light frequency when grating instruments were used, but the maximum spectral extent observable with these instruments was about 4000 cm^{-1} , and simultaneous observation of Stokes and anti-Stokes spectra for a single laser shot was impossible in the case of an extremely large spectral extent. Using spectrographs with only a wire for a filter allowed the display of Stokes and anti-Stokes SPM spectra from the same filament simultaneously, and under these conditions the maximum spectral shift on the Stokes and anti-Stokes sides was determined to be the same within 20% for maximum shifts from 2000 to 4000 cm^{-1} .

Filaments imaged on the spectrographs range in diameter from 5 to 50μ . This range of filament size was observed in every sample. The similarity of the spectra observed in different materials strongly suggests a common mechanism for all materials. In the next section, these experimental results will be shown to imply a relatively fast mechanism and be consistent with an electronic SPM model.

THEORETICAL

The general form for the nonlinear refractive index with a quadratic field dependence is

$$n(t) = n_0 + \int_{-\infty}^t \int_{-\infty}^t f(t', t'') E(t-t') E(t-t'') dt' dt'', \quad (1)$$

where n_0 is the ordinary index, E the electric field, and $f(t', t'')$ is a weighting function describing the impulse response of the index. For a single-process mechanism with relaxation time τ , $f(t', t'')$ assumes the form

$$f(t', t'') = (n_2/\tau) e^{-t'/\tau} \delta(t' - t''), \quad (2)$$

and Eq. (1) may be simplified to

$$n(t) = n_0 + \frac{n_2}{\tau} \int_{-\infty}^t e^{-(t-t')/\tau} E^2(t') dt'. \quad (3)$$

The incident laser electric field has the form

$$E_{1a}(t) = E_0 e^{-t^2/\tau^2} \cos[\omega_0 t - g(t)], \quad (4)$$

where $T = T_p / (2 \ln 2)^{1/2}$ and T_p is the intensity full width at half-maximum (FWHM) of either the entire envelope pulse or a subpicosecond component. Two-photon fluorescence measurements⁷ and the 100-cm⁻¹ spectral extent of the laser pulses imply the existence of components as short as 0.1 psec in the pulse. The phase structure is given by $g(t)$, e. g., $g(t) = \frac{1}{2} \alpha t^2$ describes a linear chirp. Treacy⁸ measured the chirp for mode-locked pulses at 1.06 μ and obtained $\alpha = 2.5 \times 10^{24}$ sec².

After an intense light beam has propagated a distance z into the material, the electric field has been distorted in phase and has the form

$$E(t) = E_0 e^{-t^2/T^2} \cos[\varphi(t)], \quad (5)$$

where the modulated instantaneous phase is

$$\varphi(t) = \omega_0 t - n(t) \omega_0 z / c. \quad (6)$$

Dispersion has been neglected.⁹ The spectral density of the phase modulated light is

$$S(\omega) = (c/4\pi) |E(\omega)|^2, \quad (7)$$

where $E(\omega)$ is the Fourier transform of $E(t)$.

The experimental results of the previous section may be used to determine an upper limit for the relaxation time τ of the index nonlinearity mechanism. Following Shimizu,² we define the instantaneous frequency $\omega(t) = \partial\varphi(t)/\partial t$ and estimate the frequency sweeps to the Stokes and anti-Stokes sides as the minimum and maximum, respectively, of $\omega(t) - \omega_0$. For unchirped pulses, these sweeps are the same and are essentially equal to

$$\Delta\omega = \omega_0 (z/c\tau^*) (n_2 E_0^2). \quad (8)$$

Here, τ^* is the shortest time in which the nonlinear index changes significantly and which provides an upper limit for the actual mechanism relaxation time. It should be noted that the quantity E^2 appearing in (3) is not averaged over several optical cycles and is not identical to the quantity $\langle E^2 \rangle$ used by Cheung *et al.*³ in their equation for the nonlinear index. These authors discussed relatively slow mechanisms that can respond only at small difference frequencies and not at optical frequencies, and their averaging is appropriate. For fast mechanisms with τ comparable to or less than $1/\omega_0$, averaging is improper and leads to the erroneous conclusion that the nonlinear index cannot change significantly over times shorter than the pulse width. There is no physical reason why an electronic mechanism for the nonlinear index cannot be driven at optical frequencies; therefore τ^* , which by definition is the shortest time the nonlinear index can react, can be much shorter than the pulse rise time. We observe typically about 4000-cm⁻¹ broadening on either side for an active length¹⁰ $z \sim 1$ cm in various materials, and $n_2 E_0^2$ is estimated to be $\lesssim 10^{-4}$ esu from Kerr-gate experiments¹¹

and from the diameters of the observed filaments. We conclude that the mechanism relaxation time must be $\lesssim 1.5 \times 10^{-14}$ sec. If a very strong chirp were present we would be forced to attribute part of the spectral extent to it and to revise our estimate of the maximum relaxation time upwards, but the chirp magnitude reported by Treacy⁸ is too small to affect the SPM spectra significantly. The presence of absorption could limit the observed spectrum. Our relaxation-time estimate would then be too high to correspond to the actual relaxation time, but this would not alter its function as an upper limit.

A pure electronic mechanism for the nonlinear index involves no translation of nuclei or rotation of atomic clusters, and is expected to have a relaxation time much less than the optical period, so $\tau < 1/\omega_0$. For this case the index can respond at optical frequencies. Hence, the averaging procedure in (3) is unnecessary, and the weighting function $(1/\tau) e^{-(t-t')/\tau}$ in (4) may be replaced by $\delta(t-t')$. The nonlinear index is simply

$$n(t) = n_0 + n_2 E_0^2 e^{-2t^2/T^2} \cos^2(\omega_0 t). \quad (9)$$

The electric field at z is given by

$$E(t) = E_0 e^{-t^2/T^2} \cos[\omega_0(t - n_0 z/c) - \beta e^{-2t^2/T^2} \cos^2(\omega_0 t)], \quad (10)$$

where $\beta = (n_2 E_0^2) (\omega_0 z/c)$. Using the Bessel-function expansions

$$\cos(y \cos \theta) = J_0(y) + 2 \sum_{k=1}^{\infty} (-1)^k J_{2k}(y) \cos 2k\theta, \quad (11a)$$

$$\sin(y \cos \theta) = 2 \sum_{k=0}^{\infty} (-1)^k J_{2k+1}(y) \cos(2k+1)\theta, \quad (11b)$$

and truncating the series to exclude third and higher harmonics which are absorbed in the experiments ($\lambda < 1770$ Å), we can rewrite $E(t)$ as

$$E(t) = E_0 e^{-t^2/T^2} \{ \cos[\omega_0 t - B(t)] J_0(B(t)) - \sin[\omega_0 t + B(t)] J_1(B(t)) \}, \quad (12a)$$

where

$$B(t) = \frac{1}{2} \beta e^{-2t^2/T^2}. \quad (12b)$$

If the primary rather than the second harmonic of the mode-locked laser had been used, it would have been necessary to retain the third-harmonic term in (12a). Spectra for the electronic mechanism were computed numerically from (12) for different values of β and the field FWHM $T_f = T_p \sqrt{2}$. The Fourier transform $E(\omega)$ was evaluated by means of a fast Fourier-Gaussian algorithm. Theoretical spectra are presented in Fig. 3 for the following

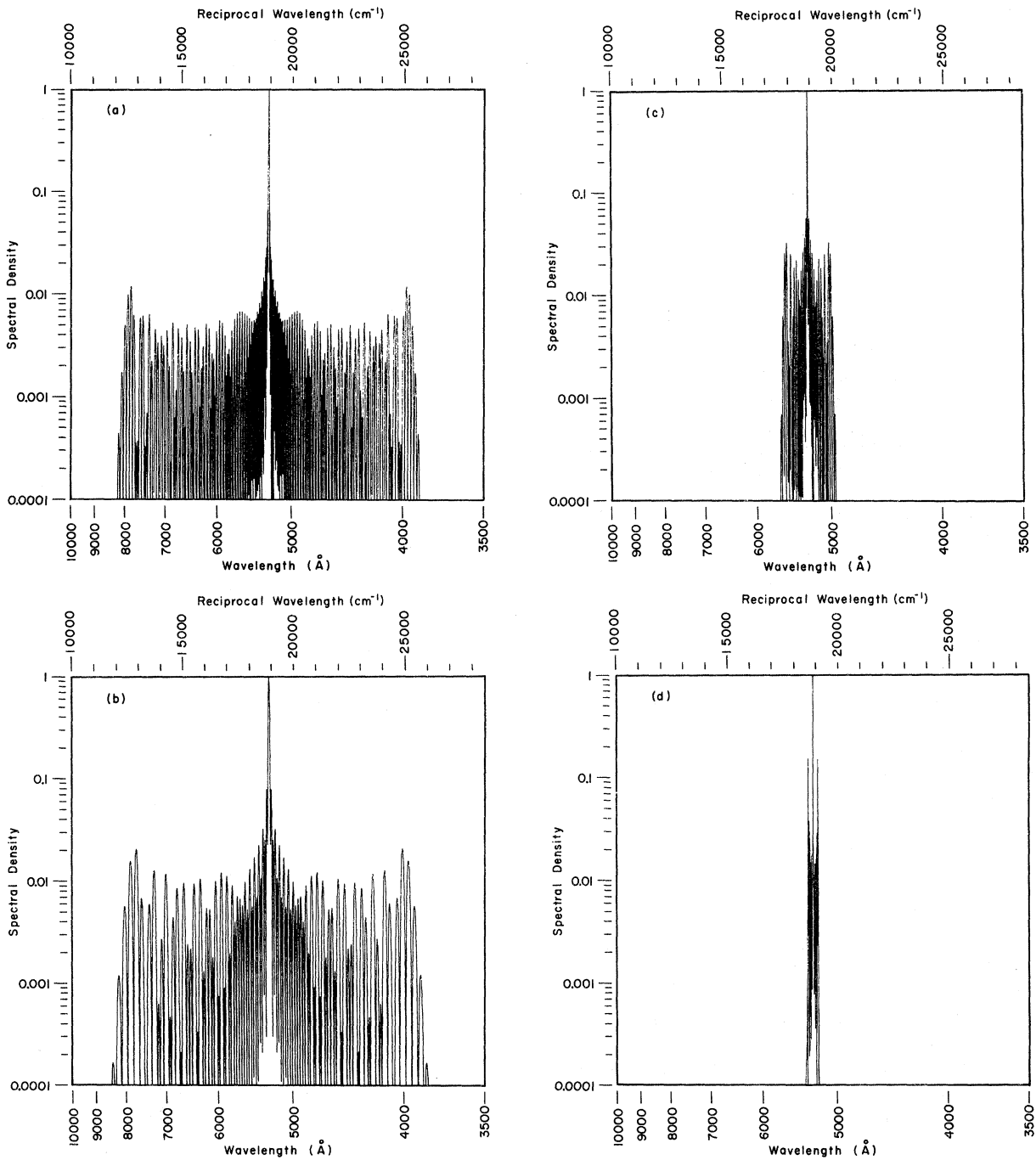


FIG. 3. Calculated SPM spectra for different laser and material parameters: (a) $\beta=120$, $T_f=0.4$ psec; (b) $\beta=60$, $T_f=0.2$ psec; (c) $\beta=30$, $T_f=0.6$ psec; (d) $\beta=60$, $T_f=4\sqrt{2}$ psec; (e) $\beta=120$, $T_f=0.6$ psec; (f) $\beta=120$, $T_f=0.6$ psec; $\alpha=2.5 \times 10^{24} \text{ sec}^{-2}$.

parameter values: Fig. 3(a), $\beta=120$, $T_f=0.4$ psec; Fig. 3(b), $\beta=60$, $T_f=0.2$ psec; Fig. 3(c), $\beta=30$, $T_f=0.6$ psec; Fig. 3(d), $\beta=60$, $T_f=4\sqrt{2}$ psec; Fig. 3(e), $\beta=120$, $T_f=0.6$ psec. A spectrum for a chirped pulse with $\beta=120$, $T_f=0.6$ psec, and $\alpha=2.5 \times 10^{24} \text{ sec}^{-2}$ is given in Fig. 3(f).

Except for the chirped spectrum, the spectra are symmetric about the input frequency, in agreement with experiment. The wings are less intense than the central peak by about a factor of 100, again in agreement with experiment. A nonperiodic structure of intensity maxima and minima are

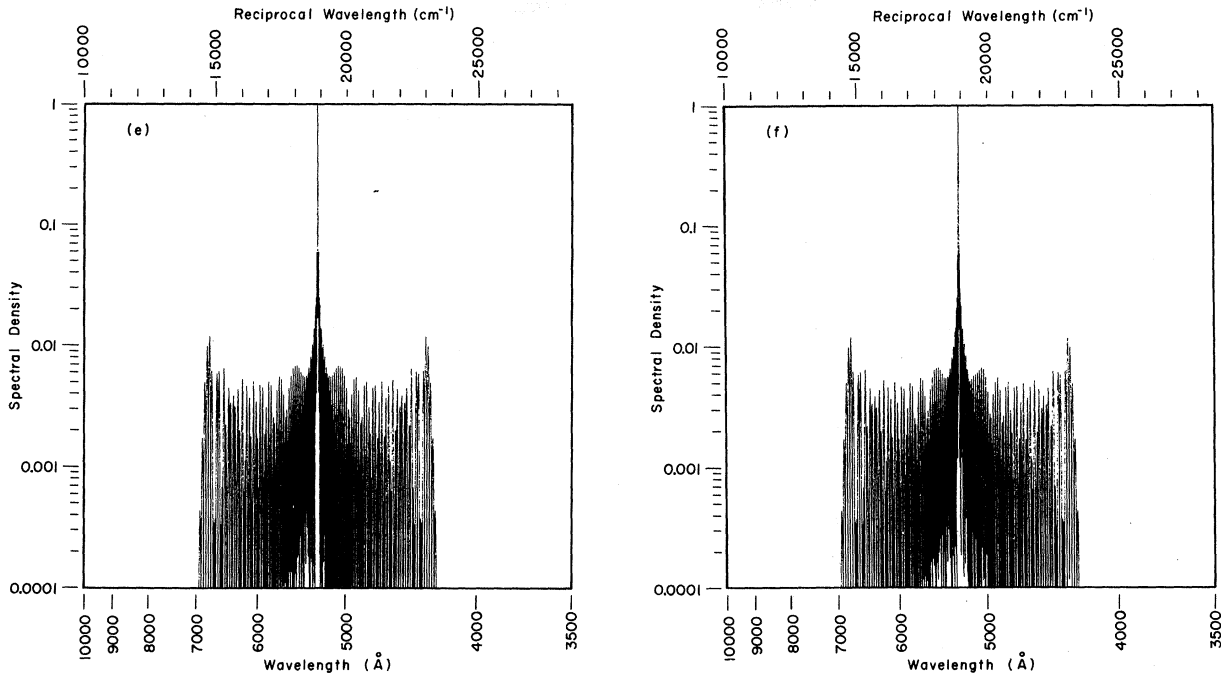


FIG. 3. Continued

obtained ranging from a few cm^{-1} to thousands of cm^{-1} depending on β and T_f .

The internal spectral structure (as distinct from the spectral extent) varies from shot to shot. One reason for this is probably the presence of more than one input pulse or subpicosecond pulse components. If the Fourier transform of each subcomponent pulse $h(t)$ is $h(\omega)$, and if the subpicosecond components of a picosecond pulse are written in the form $E(t) = \sum_n a_n h(t - t_n)$, then $E(\omega) = h(\omega) \times \sum_n a_n e^{i\omega t_n}$. The internal structure is complicated by the second factor in this last expression. Calculation of $S(\omega)$ for a subpicosecond pulse array shows that the internal structure is changed slightly but the spectral extent is not affected. The spectral extent is not given by (8), because of absorption of higher harmonics, but comparison of the spectra for various β and T_f shows that the extent is proportional to β/T_f . The chirped-pulse spectrum 3(f) is quite similar to the unchirped pulse 3(e), verifying that a reasonable chirp magnitude does not affect the spectra significantly.

Similar numerical calculations carried out under the assumptions that the mechanism has a relaxation time of the order of 1 psec (following the envelope of the pulse) and that no absorption is present resulted in quite narrow spectra ($< 500 \text{ cm}^{-1}$). An estimate from Eq. (8) of the spectral extent is in agreement with extent obtained from numerical calculations of the spectral densities if τ^* is the rise time of the pulse. An asymmetrical input laser pulse would be directly reflected in an asym-

metrical SPM spectrum.

A SPM spectrum for the case of an electronic mechanism operating together with a slower mo-

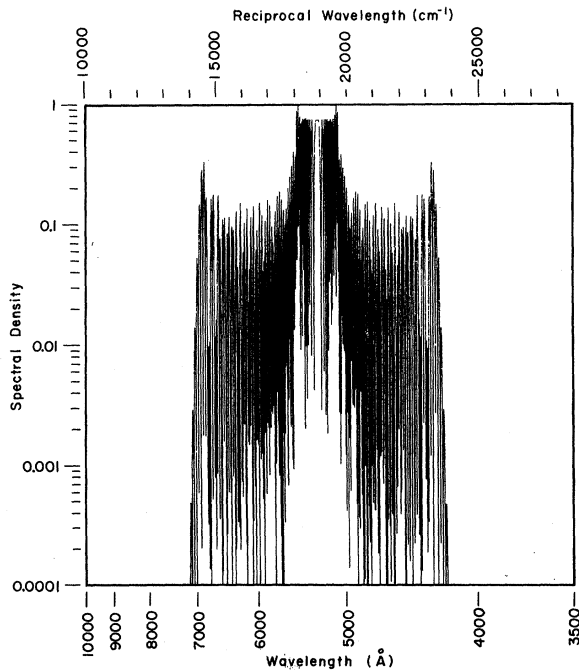


FIG. 4. Calculated SPM spectrum for an electronic and a molecular mechanism contributing to the nonlinear index: $\beta(\text{electronic}) = 120$, $T_f = 0.6 \text{ psec}$; $\beta(\text{molecular}) = 1200$, $T_f = 4\sqrt{2} \text{ psec}$.

lecular mechanism appears in Fig. 4.¹² We take the FWHM of the pulse subcomponents, 0.6 psec, as T_f .⁷ For the electronic mechanism, $\beta = 120$ and the electronic contribution to the nonlinear index is given by (9). The spectrum for this mechanism operating alone is that of Fig. 3(e). For the molecular mechanism, $\beta = 1200$ and the contribution to the nonlinear index is computed from (3) with $\tau = 2$ psec. These values of β are based on typical values for n_2 ¹² and our value for E_0^2 . By comparison of Fig. 4 with Fig. 3(e) it is seen that the spectral extent is determined almost entirely by the electronic mechanism, while the slower mechanism only affects the internal structure of the spectrum, in spite of the fact that $n_2(\text{molecular}) = 10n_2(\text{electronic})$. The electronic mechanism dominates because the spectral extent depends on β/τ^* , and in general $(\beta/\tau^*)(\text{electronic}) \gg (\beta/\tau^*)(\text{other mech-}$

anisms).

In conclusion, when intense picosecond pulses are passed through materials, our observations of SPM spectral characteristics (intensity, extent, symmetry, internal structure) are consistent with a fast relaxation time for the nonlinear index mechanism, and an electronic mechanism fits our observed SPM spectra. At the present time we can not exclude the possibility of another fast mechanism operating in individual cases, but the electronic mechanism is consistent with our observed spectra in all cases.

ACKNOWLEDGMENT

We thank Dr. A. Lempicki for helpful discussions and for his interest and encouragement during all phases of this work.

¹R. G. Brewer, Phys. Rev. Letters **19**, 8 (1967).

²F. Shimizu, Phys. Rev. Letters **19**, 1097 (1967).

³A. C. Cheung, D. M. Rank, R. Y. Chiao, and C. H. Townes, Phys. Rev. Letters **20**, 786 (1968); R. Polloni, C. A. Sacchi, and O. Svelto, *ibid.* **23**, 690 (1969).

⁴R. G. Brewer and C. H. Lee, Phys. Rev. Letters **21**, 267 (1968).

⁵R. R. Alfano and S. L. Shapiro, Phys. Rev. Letters **24**, 584 (1970); **24**, 592 (1970); **24**, 1217 (1970); Phys. Rev. A **2**, 2776 (1970); R. R. Alfano, A. Lempicki, and S. L. Shapiro, IEEE J. Quantum Electron. **7**, 416 (1971); and Gordon Conference, 1971 (unpublished) reported that (i) SRS is emitted from Nd:POCl₃ mode-locked laser and (ii) frequency broadening extending from 1.06 to 0.33 μ and third-harmonic generation at 0.353 μ are emitted from a mode-locked Nd:glass laser. The broadening is approximately exponential in shape with an intensity at 0.4 $\mu \sim 10^{-10}$ less than at 1.06 μ .

⁶R. Hellwarth, A. Owyong, and N. George, Phys. Rev. A **4**, 2342 (1971).

⁷S. L. Shapiro and M. A. Duguay, Phys. Letters **28A**, 698 (1969).

⁸E. B. Treacy, Phys. Letters **28A**, 34 (1968).

⁹The SPM pulse has been shown to be an ideal tool for picosecond spectroscopy [R. R. Alfano and S. L. Shapiro, Chem. Phys. Letters **8**, 631 (1971)]. A SPM pulse after propagating a distance z into a material becomes broadened due to dispersion, thereby washing out the subpicosecond-pulse array—the red frequency components move to the leading edge and the blue to the trailing edge of the picosecond envelope. A SPM pulse of duration 0.3 psec with a total spectral extent of 8000 cm^{-1} will broaden to ~ 6 psec after propagating through 4 cm of BK-7 glass.

¹⁰The interaction length for the SPM process in, for example, BK-7 glass is ≥ 2 mm for the spectral components within the anti-Stokes 4000- cm^{-1} frequency sweep for the 5300- \AA subpicosecond pulse of 0.3-psec duration.

¹¹M. A. Duguay and J. W. Hansen, Appl. Phys. Let-

ters **15**, 192 (1969); R. R. Alfano and S. L. Shapiro (private communication).

¹²There are many mechanisms contributing to the nonlinear-refractive-index coefficient n_2 for picosecond light pulses. Their magnitudes range from $\sim 10^{-11}$ to 10^{-14} esu and temporal responses range from $\sim 10^{-11}$ to 10^{-16} sec depending on the mechanism. The nonlinear refractive index for materials with different mechanisms can take the form $\delta n(t) = \sum_j \delta n_j(E_0, T_p, \tau_j, t)$, where the index j defines the various mechanisms (electronic, rocking, redistribution, orientational, etc.) and τ_j is the individual response time. The spectral amplitude for a plane wave in a material having many mechanisms operative is the convolution of spectra for the separate processes, i.e., for three mechanisms:

$$E(\omega) = \int_{-\infty}^{\infty} \mathcal{F}_1(\omega_1) \mathcal{F}_2(\omega_2 - \omega_1) \mathcal{F}_3(\omega - \omega_2) d\omega_1 d\omega_2,$$

where $\mathcal{F}_j(\omega)$ is the Fourier transform of $f_j(t)$ and $f_1(t) = E_0(t)e^{i6n_1\omega_0 t/c}$, $f_2(t) = e^{i6n_2\omega_0 t/c}$, and $f_3(t) = e^{i6n_3\omega_0 t/c}$. A table of calculated values for n_2 for different mechanisms in various materials may be found in S. Kielich and S. Wozniak, Acta Phys. Polon. A **39**, 233 (1971). The value of n_2 for argon and krypton is measured to be 6×10^{-14} and 1.36×10^{-13} esu, respectively, by A. D. Buckingham and D. A. Dunmur, Trans. Faraday Soc. **64**, 1776 (1968). The value of n_2 for BK-7 glass is measured to be 3.2×10^{-13} esu by C. Wang and E. L. Baardsen [Phys. Rev. B **1**, 2827 (1970)] by third-harmonic generation, and 2.6×10^{-13} esu by Duguay and J. Hansen [Natl. Bur. Std. (US) Publ. No. 341 (1970)] by the optical Kerr effect. For a 0.1-psec input pulse, comparison of the calculated spectra for the electronic mechanism and a molecular mechanism with response time 0.05 psec with the same values of n_2 ($\beta = 30$) shows that the electronic spectrum dominates the spectral extent by a factor of $\frac{5}{3}$. If a more typical value of τ of 0.5 psec is chosen for the response time of the molecular mechanism, then the electronic mechanism produces a spectral extent $\frac{50}{3}$ as large.

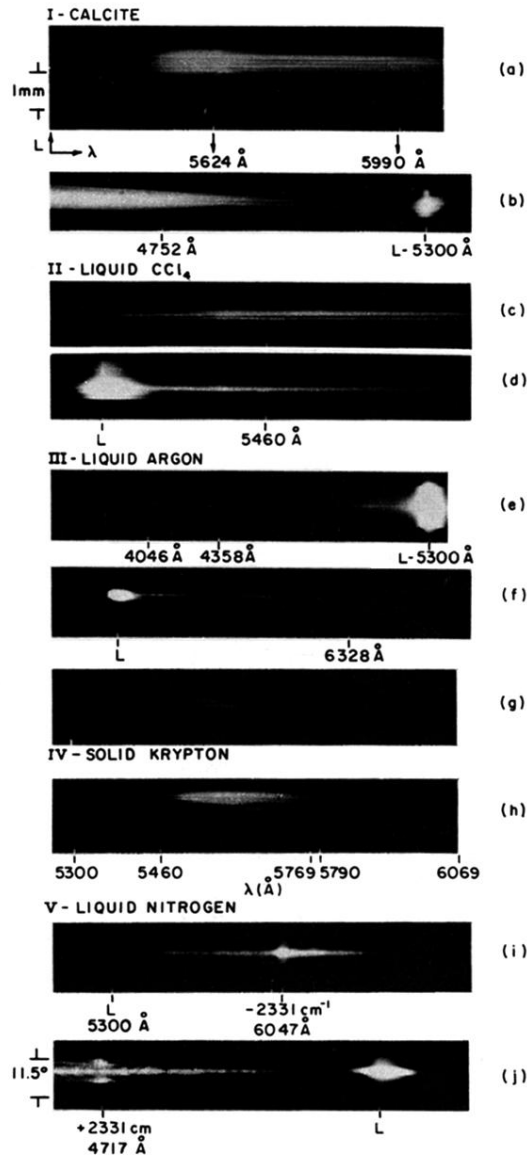


FIG. 2. SPM spectra observed when intense, $5300\text{-}\text{\AA}$, psec laser pulses are passed through the following material. I: Calcite—length $l=5$ cm. (a) Stokes filter $F(2, 3-67)$ and (b) anti-Stokes $F(2, 5-60)$ spectra. II: Liquid CCl_4 — $l=4$ cm. (c) Stokes $F(4, 3-68)$ and (d) Stokes $F(1, 3-68)$ spectra. III: Liquid argon— $l=12$ cm. (e) anti-Stokes $F(5-61)$, (f) Stokes, $F(3-67)$, and (g) Stokes $F(3, 3-67)$ spectra. The beam is focused into the sample with $f=25$ -cm lens (the beam diameter is measured to be $\sim 300 \mu$ at the focal point); IV: Solid krypton— $l=12$ cm. (h) Stokes $F(3, 3-67)$ spectra. The beam is focused with $f=25$ -cm lens. V: Liquid nitrogen— $l=7$ cm. (i) Stokes $F(3-67)$ and (j) anti-Stokes $F(5-60, 5-61)$ angular emission spectra. Photograph (i) displays stimulated Raman emission and axial SPM and (j) displays an anti-Stokes ring and axial SPM.